Maximum Angle Method for Determining Mixed Layer Depth from Seaglider Data

Peter C. Chu and Chenwu Fan
Department of Oceanography
Naval Postgraduate School
Monterey, CA 93940, USA

Report Documentation Page

Form Approved
OMB No. 0704-0188

1. REPORT DATE	2. REPORT TYPE	3. DATES COVERED
2010		**00-00-2010 to 00-00-2010**

4. TITLE AND SUBTITLE	5a. CONTRACT NUMBER
Maximum Angle Method for Determining Mixed Layer Depth from Seaglider Data	5b. GRANT NUMBER
	5c. PROGRAM ELEMENT NUMBER
6. AUTHOR(S)	5d. PROJECT NUMBER
	5e. TASK NUMBER
	5f. WORK UNIT NUMBER
7. PERFORMING ORGANIZATION NAME(S) AND ADDRESS(ES) **Naval Postgraduate School,Department of Oceanography,Monterey,CA,93943**	8. PERFORMING ORGANIZATION REPORT NUMBER
9. SPONSORING/MONITORING AGENCY NAME(S) AND ADDRESS(ES)	10. SPONSOR/MONITOR'S ACRONYM(S)
	11. SPONSOR/MONITOR'S REPORT NUMBER(S)

12. DISTRIBUTION/AVAILABILITY STATEMENT
Approved for public release; distribution unlimited

13. SUPPLEMENTARY NOTES
Journal of Oceanography, Oceanographic Society of Japan, resubmitted after revision

14. ABSTRACT

A new maximum angle method has been developed to determine surface mixed-layer (a 19 general name for isothermal/constant-density layer) depth from profile data. It has three steps 20 (1) fitting the profile data with a first vector (pointing downward) from a depth to an upper level 21 and a second vector (pointing downward) from that depth to a deeper level, (2) identifying the 22 angle (varying with depth) between the two vectors, (3) finding the depth (i.e., the mixed layer 23 depth) with maximum angle between the two vectors. Temperature and potential density profiles 24 collected from two seagliders in the Gulf Stream near Florida coast during 14 November ? 5 25 December 2007 were used to demonstrate its capability. The quality index (1.0 for perfect 26 identification) of the maximum angle method is about 0.96. The isothermal layer depth is 27 generally larger than the constant-density layer depth, i.e., the barrier layer occurs during the 28 study period. Comparison with the existing difference, gradient, and curvature criteria shows the 29 advantage of using the maximum angle method. Uncertainty due to varying threshold using the 30 difference method is also presented.

15. SUBJECT TERMS

16. SECURITY CLASSIFICATION OF:			17. LIMITATION OF ABSTRACT	18. NUMBER OF PAGES	19a. NAME OF RESPONSIBLE PERSON
a. REPORT	b. ABSTRACT	c. THIS PAGE			
unclassified	**unclassified**	**unclassified**	**Same as Report (SAR)**	**33**	

Abstract

A new maximum angle method has been developed to determine surface mixed-layer (a general name for isothermal/constant-density layer) depth from profile data. It has three steps: (1) fitting the profile data with a first vector (pointing downward) from a depth to an upper level and a second vector (pointing downward) from that depth to a deeper level, (2) identifying the angle (varying with depth) between the two vectors, (3) finding the depth (i.e., the mixed layer depth) with maximum angle between the two vectors. Temperature and potential density profiles collected from two seagliders in the Gulf Stream near Florida coast during 14 November – 5 December 2007 were used to demonstrate its capability. The quality index (1.0 for perfect identification) of the maximum angle method is about 0.96. The isothermal layer depth is generally larger than the constant-density layer depth, i.e., the barrier layer occurs during the study period. Comparison with the existing difference, gradient, and curvature criteria shows the advantage of using the maximum angle method. Uncertainty due to varying threshold using the difference method is also presented.

1. Introduction

Transfer of mass, momentum, and energy across the bases of surface isothermal and constant-density layers provides the source for almost all oceanic motions. Underneath the surface constant-density and isothermal layers, there exist layers with strong vertical gradients such as the pycnocline and thermocline. The mixed layer depth (MLD) (a general name for isothermal/constant-density layer depth) is an important parameter which influences the evolution of the sea surface temperature. The isothermal layer depth (H_T) is not necessarily identical to the constant-density layer depth (H_D) due to salinity stratification. There are areas of the World Ocean where H_T is deeper than H_D (Lindstrom et al., 1987; Chu et al., 2002; de Boyer Montegut et al., 2007). The layer difference between H_D and H_T is defined as the barrier layer. For example, barrier layer was observed from a seaglider in the western North Atlantic Ocean near the Florida coast (30.236^{o}N, 78.092^{o}W) at GMT 23:20 on November 19, 2007 (Fig. 1). The barrier layer thickness (BLT) is often referred to as the difference, BLT = H_T - H_D. Less turbulence in the barrier layer than in the constant-density layer due to strong salinity stratification isolates the constant-density layer water from cool thermocline water. This process regulates the ocean heat budget and the heat exchange with the atmosphere, and in turn affects the climate.

Objective and accurate identification of H_T and H_D is important for the determination of barrier layer occurrence and its climate impact. Three types of criteria (difference, gradient, and curvature) are available for identifying H_T from profiling data. The difference criterion requires the deviation of T (or ρ) from its near surface (i.e., reference level) value to be smaller than a certain fixed value. The gradient criterion requires $\partial T/\partial z$ (or $\partial \rho/\partial z$) to be smaller than a certain

fixed value. The curvature criterion requires $\partial^2 T/\partial z^2$ (or $\partial^2 \rho/\partial z^2$) to be maximum at the base of mixed layer ($z = -H_D$).

The difference and gradient criteria are subjective. For example, the criterion for determining H_T for temperature varies from 0.8°C (Kara et al., 2000), 0.5°C (Wyrtki, 1964) to 0.2°C (de Boyer Montegut et al., 2004). The reference level changes from near surface (Wyrtki, 1964) to 10 m depth (de Boyer Montegut et al., 2004). The criterion for determining H_D for potential density varies from 0.03 kg/m^3 (de Boyer Montegut et al., 2004), 0.05 kg/m^3 (Brainerd and Gregg, 1995), to 0.125 kg/m^3 (Suga et al., 2004). Defant (1961) was among the first to use the gradient method. He used a gradient of 0.015°C/m to determine H_T for temperature of the Atlantic Ocean; while Lukas and Lindstrom (1991) used 0.025°C/m. The curvature criterion is an objective method (Chu et al, 1997, 1999, 2000; Lorbacher et al., 2006); but is hard to use for profile data with noise (even small), which will be explained in Section 5. Thus, it is urgent to develop a simple objective method for determining MLD with the capability of handling noisy data.

In this study, a new maximum angle method has been developed to determine H_T and H_D and the gradients of the thermocline and pycnocline from profiles and tested using data collected by two seagliders of the Naval Oceanographic Office in the Gulf Stream region near the Florida coast during 14 November – 5 December 2007, with comparison to the existing methods. The results demonstrate its capability. The outline of this paper is listed as follows. Section 2 describes hydrographic data from the two seagliders. Section 3 presents the methodology. Sections 4 and 5 compare the maximum angle method with the existing methods. Section 6

shows the occurrence of barrier layer in the western North Atlantic Ocean. Section 7 presents the conclusions.

2. Seaglider Data

Two seagliders were deployed in the Gulf Stream region near the Florida coast by the Naval Oceanographic Office (Mahoney et al., 2009) from two nearby locations on 14 November 2007 with one at (79.0^o W, 29.5^{o}N) (Seaglider-A) and the other at (79.0^o W, 29.6^{o}N) (Seaglider-B) (Fig. 2). Seaglider-A (solid curve) moved toward northeast to (78.1^{o}W, 30.25^{o}N), turned anticyclonically toward south and finally turned cyclonically at (78.4^{o}W, 29.6^{o}N). Seaglider-B (dashed curve) moved toward north to (79.0^{o}W, 30.0^{o}N), turned toward northeast and then anticyclonically, and finally turned cyclonically.

The seaglider goes up and down in oblique direction, not vertical. Data collected during a downward-upward cycle are divided into two parts with the first one from the surface to the deepest level and the second one from the deepest level to the surface. Each part represents an individual profile with the averaged longitude and latitude of the data points as the horizontal location. Such created temperature and potential density profile data went through quality control procedures; such as, min-max check (e.g., disregarding any temperature data less than –2^{o}C and greater than 35^{o}C), error anomaly check (e.g., rejecting temperature and salinity data deviating more than 3 standard deviations from climatology), seaglider-tracking algorithm (screening out data with obvious seaglider position errors), max-number limit (limiting a maximum number of observations within a specified and rarely exceeded space-time window), and buddy check (tossing out contradicting data). The climatological data set used for the quality control is the Navy's Generalized Digital Environmental Model (GDEM) climatological

temperature and salinity data set. After the quality control, 514 profiles of (T, ρ) are available with 265 profiles from Seaglider-A and 249 profiles from Seaglider-B. The vertical resolution of the profile varies from less than 1 m for upper 10 m, to approximately 1-3 m below 10 m depth. All the profiles are deeper than 700 m and clearly show the existence of layered structure: isothermal (constant-density) layer, thermocline (pycnocline), and deep layer.

3. Determination of (H_T, H_D)

Let potential density and temperature profiles be represented by [$\rho(z_k)$, $T(z_k)$]. Here, k increases downward with k = 1 at the surface or nearest to the surface and K the total number of the data points for the profile. The potential density profile is taken for illustration of the new methodology. Let (ρ_{max} , $\rho_{\min}$) be the maximum and minimum of the profile $\rho(z_k)$. Starting from z_1 downward, depth with $\rho_{\min}$ (z_{min}) and depth with ρ_{max} (z_{max}) are found. Without noise, z_{min} should be z_1 and z_{max} should be z_K. The vertical density difference, $\Delta\rho = \rho_{max} - \rho_{\min}$, represents the total variability of potential density. Theoretically, the variability is 0 in the constant-density layer and contains large portion in the pycnocline. It is reasonable to identify the main part of the pycnocline between the two depths: $z_{(0.1)}$ with $0.1\Delta\rho$ and $z_{(0.7)}$ with of $0.7\Delta\rho$ relative to $\rho_{\min}$ (Fig. 3). Let n be the number of the data points between $z_{(0.1)}$ and $z_{(0.7)}$ and $m = \min(n, 20)$.

At depth z_k (marked by a circle in Fig. 4), a first vector ($\mathbf{A}_1$, downward positive) is constructed with linear polynomial fitting of the profile data from z_{k-j} to z_k with

$$j = \begin{cases} k-1, & \text{for} \quad k \le m \\ m, & \text{for } k > m \end{cases}. \qquad (1)$$

A second vector ($\mathbf{A}_2$, pointing downward) from one point below that depth (i.e., z_{k+1}) is constructed to a deeper z_{k+m}. The dual- linear fitting can be represented by

$$\rho(z) = \begin{cases} c_k^{(1)} + G_k^{(1)} z, & z = z_{k-j}, z_{k-j+1}, \ldots z_k \\ c_k^{(2)} + G_k^{(2)} z, & z = z_{k+1}, \ldots z_{k+m} \end{cases}, \qquad (2)$$

where $c_k^{(1)}$, $c_k^{(2)}$, $G_k^{(1)}$, $G_k^{(2)}$ are the fitting coefficients.

At the constant-density (isothermal) layer depth, the angle θ_k reaches its maximum value if z_k is the MLD (see Fig. 4a), and smaller if z_k is inside (Fig. 4b) or outside (Fig. 4c) of the mixed layer. Thus, the maximum angle principle can be used to determine the mixed (or isothermal) layer depth,

$$\theta_k \to \max, \quad H_D = -z_k.$$

In practical, the angle θ_k is hard to calculate, so tan θ_k is used instead, i.e.,

$$\tan\theta_k \to \max, \quad H_D = -z_k, \quad G^{(1)} = G_k^{(1)}, \quad G^{(2)} = G_k^{(2)}, \qquad (3)$$

where $G^{(1)} \approx 0$, is the vertical gradient in the mixed layer; and $G^{(2)}$ is the vertical gradient in the thermocline (pycnocline). With the given fitting coefficients $G_k^{(1)}$, $G_k^{(2)}$, tan θ_k can be easily calculated by

$$\tan\theta_k = \frac{G_k^{(2)} - G_k^{(1)}}{1 + G_k^{(1)} G_k^{(2)}}. \qquad (4)$$

The maximum angle method [i.e., (1)- (4)] was used to calculate H_T and H_D from 514 pairs of temperature and potential density profiles from the two seagliders. With high vertical resolution of the data, H_T and H_D can be determined for all profiles. The potential density profile at the station (shown in Fig. 1) located at (30.236^{o}N, 78.092^{o}W) is taken as an example for illustration (Fig. 5a). At $z = -H_D$, tan θ_k has maximum value (Fig. 5b).

Advantage of the maximum angle method is described as follows. Different from the existing methods, the maximum angle method not only uses the main feature (vertically uniform) of mixed layer such as in the difference and gradient criteria, but also uses the main characteristics (sharp gradient) below the mixed layer (see Fig. 3). After MLD is determined, the vertical gradient of the thermocline (pycnocline), $G^{(2)}$, is also calculated. The dataset of $G^{(2)}$ is useful for studying the heat and salt exchange between the ocean upper and lower layers. Besides, the maximum angle method is less subjective comparing to the existing methods. The only external parameters (10% and 70%) are used to determine $z_{0.1}$ and $z_{0.7}$, and in turn to determine the length of the vectors $\mathbf{A}_1$ and $\mathbf{A}_2$.

Disadvantage of the maximum angle method is due to the use of two linear regressions [see Eq(2)]. Reliable regression needs sufficient sample size. For profiles with very few data points (low resolution), the maximum angle method might not work. The seaglider data described in Section 2 are high-resolution profiles, and therefore are perfect for the test of the maximum angle method.

4. Comparison between Maximum Angle and Threshold Methods

Lorbacher et al. (2006) proposed a quality index (QI)

$$\mathrm{QI} = 1 - \frac{\mathrm{rmsd}\left(\rho_k - \hat{\rho}_k\right)|_{(H_1, H_D)}}{\mathrm{rmsd}\left(\rho_k - \hat{\rho}_k\right)|_{(H_1, 1.5\times H_D)}}, \qquad (5)$$

to evaluate various schemes for H_D (or H_T) determination. Here, $\rho_k = \rho(z_k)$, is the observed profile, $\hat{\rho}_k =$ mean potential density between z_1 and $z = -H_D$. For a perfect identification, $\mathrm{rmsd}\left(\rho_k - \hat{\rho}_k\right)|_{(H_1, H_D)} = 0$, QI = 1. The higher the QI, the more reliable identification of MLD

would be. Usually, H_D is defined with certainty if QI > 0.9; can be determined with uncertainty if 0.9 > QI > 0.5; and can't be identified if QI < 0.5.

Capability of the maximum angle method is demonstrated through comparison with the existing threshold method. Since the MLD based on a difference criterion is more stable than the MLD based on a gradient criterion, which requires sharp gradient-resolved profiles (Brainerd and Gregg, 1995), the difference threshold method is used for the comparison. Four sets of isothermal depth were obtained from 514 temperature profiles of the two seagilders using the maximum angle method, 0.2^{o}C (de Boyer Montegut et al., 2004), 0.5^{o}C (Monterey and Levitus, 1997), and 0.8^{o}C (Kara et al., 2000) thresholds. Fig. 6 shows the histograms of 514 H_T -values for the four methods. Difference of the histograms among 0.2^{o}C (Fig. 6b), 0.5^{o}C (Fig. 6c), and 0.8^{o}C (Fig. 6d) thresholds implies uncertainty using the difference method. Table-1 shows the statistical characteristics of H_T determined by the four methods. The mean (median) H_T value is 77.2 m (73.2 m) using the maximum angle method. For the difference method, it increases with the value of the threshold from 71.9 m (71.8 m) using 0.2^{o}C, 82.0 m (77.9 m) using 0.5^{o}C, to 87.6 m (82.9 m) using 0.8^{o}C.

The Gaussian distribution has skewness of 0 and kurtosis of 3. Obviously, the four histograms show non-Gaussian features. H_T is positively skewed when it is identified using all the four methods. The skewness of H_T is sensitive to the thresholds: 0.21 using 0.2^{o}C, 1.13 using 0.5^{o}C, and 1.25 using 0.8^{o}C. It is 0.69 using the maximum angle method. The kurtosis of H_T is larger than 3 for all the four methods and sensitive to the thresholds: 3.48 using 0.2^{o}C, 4.46 using 0.5^{o}C, and 4.35 using 0.8^{o}C. It is 3.80 using the maximum angle method.

The histograms of 514 QI –values are negatively skewed for the four methods (Fig. 7). Most QI-values are larger than 0.980 with a mean value of 0.965 using the maximum angle method (Fig. 7a) and are lower using the threshold method (Figs. 6b-d). The mean QI-value reduces from 0.881 with 0.2^{o}C threshold (Fig. 7b), 0.858 with 0.5^{o}C threshold (Fig. 7c), to 0.833 with 0.8^{o}C threshold (Fig. 7d).

Uncertainty of the difference method from one to another threshold can be identified by computing the relative root-mean square difference (RRMSD),

$$\mathrm{RRMSD} = \frac{1}{\bar{H}^{(1)}} \sqrt{\frac{1}{N} \sum_{i=1}^{N} (H_i^{(2)} - H_i^{(1)})^2} \ , \qquad (6)$$

where N = 514, is the number of the seaglider profiles; ($H_i^{(1)}$, $H_i^{(2)}$, i = 1, 2, …, N) are two sets of MLD identified by the difference method using two different criteria. The RRMSD of H_T is 20.1% between 0.2^{o}C and 0.5^{o}C thresholds, 28.5% between 0.2^{o}C and 0.8^{o}C thresholds, and 10.0% between 0.5^{o}C and 0.8^{o}C thresholds.

Similarly, four sets of constant-density depth were obtained from 514 potential density profiles of the two seagilders using the maximum angle method, 0.03 kg/m^3 (de Boyer Montegut et al., 2004), 0.05 kg/m^3 (Brainerd and Gregg, 1995), and 0.125 kg/m^3 (Monterey and Levitus, 1997) thresholds. Fig. 8 shows the histograms of 514 H_D -values for the four methods. H_D is positively skewed when it is identified using the maximum angle method. Difference of the histograms among 0.03 kg/m^3 (Fig. 8b), 0.05 kg/m^3 (Fig. 8c), to 0.125 kg/m^3 (Fig. 8d) threshold implies uncertainty in the difference method. Table-2 shows the statistical characteristics of H_D determined by the four methods. The mean (median) H_D value is 73.2 m (70.4 m) using the maximum angle method. It increases with the value of the threshold from 53.3 m (60.9 m) using

0.03 kg/m^3, 59.3 m (66.2 m) using 0.05 kg/m^3, to 68.0 m (71.6 m) using 0.125 kg/m^3. The skewness of H_D is slightly positive (0.28) when it is identified using the maximum angle method and slightly negative when it is identified using the threshold method. The negative skewness enhances with the threshold from -0.06 using 0.03 kg/m^3, -0.24 using 0.05 kg/m^3, to -0.59 using 0.125 kg/m^3. The kurtosis of H_D is 4.32 using the maximum angle method, and varies with the threshold when the difference method is used. It is 2.37 using 0.03 kg/m^3, 2.74 using 0.05 kg/m^3, and 3.67 using 0.125 kg/m^3.

The histograms of 514 QI –values are negatively skewed for the four methods (Fig. 9). Most QI-values are larger than 0.980 with a mean value of 0.966 for the maximum angle method (Fig. 9a) and are lower using the threshold method (Figs. 8b-d) comparing to the maximum angle method. The mean QI-value reduces from 0.837 with 0.03 kg/m^3 threshold (Fig. 9b), 0.859 with 0.05 kg/m^3 threshold (Fig. 9c), and 0.872 with 0.125 kg/m^3 threshold (Fig. 9d). The RRMSD of H_D is 29.3% between 0.03 kg/m^3 and 0.05 kg/m^3 thresholds, 44.7% m between 0.03 kg/m^3 and 0.125 kg/m^3 thresholds, and 27.8% between 0.05 kg/m^3 and 0.125 kg/m^3 thresholds.

5. Comparison between Maximum Angle and Curvature Methods

Both curvature and maximum angle methods are objective. To illustrate the superiority of the maximum angle method, an analytical temperature profile with H_T of 20 m is constructed

$$T(z)=\begin{cases} 21^oC, & \text{-20 m} < z \le \text{0 m} \\ 21^oC+0.25^oC\times(z+20\text{ m}), & \text{-40 m} < z \le \text{-20 m} \\ 7^oC+9^oC\times\exp\left(\dfrac{z+40\text{ m}}{50\text{ m}}\right), & \text{-100 m} \le z \le \text{-40 m.} \end{cases} \quad (7)$$

This profile was discretized with vertical resolution of 1 m from the surface to 10 m depth and of 5 m below 10 m depth. The discrete profile was smoothed by 5-point moving average to remove the sharp change of the gradient at 20 m and 40 m depths. The smoothed profile data [$T(z_k)$] is shown in Fig. 10a.

The second-order derivatives of $T(z_k)$ versus depth is computed by nonhomogeneous mesh difference scheme,

$$\frac{\partial^2 T}{\partial z^2}\Big|_{z_k} \approx \frac{1}{z_{k+1}-z_{k-1}}\left(\frac{T_{k+1}-T_k}{z_{k+1}-z_k}-\frac{T_k-T_{k-1}}{z_k-z_{k-1}}\right), \qquad (8)$$

Here, k = 1 refers to the surface, with increasing values indicating downward extension of the measurement. Eq.(8) shows that we need two neighboring values, T_{k-1} and T_{k+1}, to compute the second-order derivative at z_k . For the surface and 100 m depth, we use the next point value, that is,

$$\frac{\partial^2 T}{\partial z^2}\Big|_{z=0}=\frac{\partial^2 T}{\partial z^2}\Big|_{z=-1\text{ m}}, \quad \frac{\partial^2 T}{\partial z^2}\Big|_{z=-100\text{ m}}=\frac{\partial^2 T}{\partial z^2}\Big|_{z=-95\text{ m}}. \qquad (9)$$

Fig. 10b shows the calculated second-order derivatives from the profile data listed in Table 1. Similarly, tan θ_k is calculated using Eq.(4) for the same data profile (Fig. 10c). For the profile data without noise, both the curvature method (i.e., depth with minimum $\partial^2 T/\partial z^2$, see Fig. 10b) and the maximum angle method [i.e., depth with max (tan θ), see Fig. 10c)] identified the isothermal depth, i.e., H_T = 20 m.

One thousand 'contaminated' temperature profiles are generated by adding random noise with mean of zero and standard deviation of 0.02°C (generated by MATLAB) to the original profile data at each depth. An example profile is shown in Fig. 11a, as well as the second order derivative ($\partial^2 T/\partial z^2$) and tan θ. Since the random error is so small (zero mean, 0.02°C standard

deviation, within the instrument's accuracy), we may not detect the difference between Fig. 10a and Fig. 11a by eyes. However, the isothermal depth is 9 m (error of 11 m) using the curvature method (Fig. 11b) and 20 m (Fig. 11d) using the maximum angle method.

Usually, the curvature method requires smoothing for noisy data (Chu, 1999; Lorbacher et al., 2006). To evaluate the usefulness of smoothing, a 5-point moving average was applied to the 1000 "contaminated" profile data. For the profiles (Fig. 11a) after smoothing, the second derivatives were again calculated for the smoothed profiles. The isothermal depth identified for the smoothed example profile is 8 m (Fig. 11c). Performance for the curvature method (with and without smoothing) and the maximum angle method is evaluated with the relative root-mean square error (RRMSE),

$$\mathrm{RRMSE} = \frac{1}{H_T^{ac}} \sqrt{\frac{1}{N} \sum_{i=1}^{N} (H_T^{(i)} - H_T^{ac})^2} \,, \qquad (10)$$

where H_T^{ac} (= 20 m) is for the original temperature profile (Fig. 10a); N (= 1000) is the number of "contaminated" profiles; and $H_T^{(i)}$ is the calculated for the i-th profile. Table 3 shows the frequency distributions and RRMSEs of the calculated isothermal depths from the "contaminated" profile data using the curvature method (without and with 5 point-moving average) and the maximum angle method without smoothing. Without 5-point moving average, the curvature method identified only 6 profiles (out of 1000 profiles) with H_T of 20 m, and the rest profiles with H_T ranging relatively evenly from 1 m to 10 m. The RRMSE is 76%. With 5-point moving average, the curvature method identified 413 profiles with H_T of 20 m, 164 profiles with H_T of 15 m, 3 profiles with H_T of 10 m, and the rest profiles with H_T ranging relatively evenly from 2 m to 8 m. The RRMSE is 50%. However, without 5-point moving

average, the maximum angle method identified 987 profiles with H_T of 20 m, and 13 profiles with H_T of 15 m. The RRMSE is less than 3%.

6. Existence of Barrier Layer

With H_D and H_T, the BLT is easily calculated from all 514 profiles. BLT is plotted versus time in Fig. 12a (Seaglider-A) and Fig. 12b (Seaglider-B) using the maximum angle method. These two figures show a rather frequent occurrence of barrier layer in the western North Atlantic. For example, among 265 stations from Seaglider-A, there are 176 stations where barrier layer occurs. The barrier layer occur in 66.4%. The BLT has a maximum value of 30.0 m on 30 November 2007. Among 249 stations from Seaglider-B, there are 131 stations where barrier layer occurs. The barrier layer occurs in 52.6%. In this $1^o \times 2^o$ area, variation of the BLT has complex pattern and intermittent characteristics.

From Tables 1 and 2, the mean values of H_T and H_D are 77.2 m and 73.2 m, which lead to the mean BLT of 4.0 m. When the difference method is used, identification of BLT depends on the threshold. For example, de Boyer Montegut et al. (2004) used 0.2^oC and 0.03 kg/m^3. From Tables 1 and 2, the mean values of H_T and H_D are 71.9 m and 53.3 m, which lead to the mean BLT of 18.6 m. Monterey and Levitus (1997) used 0.5^oC and 0.125 kg/m^3. From Tables 1 and 2, the mean values of H_T and H_D are 82.0 m and 68.0 m, which lead to the mean BLT of 14.0 m. Comparing the existing difference methods, the barrier layer has less chance to occur using the maximum angle method.

7. Conclusions

A new maximum angle method is proposed in this study to identify isothermal and constant-density layer depths. First, two vectors (both pointing downward) are obtained using

linear fitting. Then, the tangent of the angle (tan θ) between the two vectors is calculated for all depth levels. Next, the isothermal (or constant-density) depth which corresponds to the maximum value of (tan θ) is found. Two features make this method attractive: (a) less subjective and (b) capability to process noisy data. The temperature and potential density profiles collected from two seagliders in the Gulf Stream near Florida coast during 14 November – 5 December 2007 were used for evaluating the new algorithm. With high quality indices (QI ~ 96%), the maximum angle method not only identify H_D and H_T, but also the potential density (temperature) gradient [$G^{(2)}$] below $z = -H_D$ ($z = -H_T$). Weakness of the maximum angle method is due to the sample size requirement of the regression. For low resolution profiles, the maximum angle method might not be suitable.

Uncertainty in determination of (H_T, H_D) due to different thresholds is demonstrated using the same seaglider data. Histogram of H_T (H_D) changes evidently when different thresholds are used: 0.2^{o}C (0.03 kg/m^3), 0.5^{o}C (0.05 kg/m^3), and 0.8^{o}C (0.125 kg/m^3). The RRMSD of H_T is 20.1% between 0.2^{o}C and 0.5^{o}C thresholds, 28.5% between 0.2^{o}C and 0.8^{o}C thresholds, and 10.0% between 0.5^{o}C and 0.8^{o}C thresholds. The RRMSD of H_D is 29.3% between 0.03 kg/m^3 and 0.05 kg/m^3 thresholds, 44.7% m between 0.03 kg/m^3 and 0.125 kg/m^3 thresholds, and 27.8% between 0.05 kg/m^3 and 0.125 kg/m^3 thresholds. Such large values of RRMSD make the difference method unreliable.

Acknowledgments

The Naval Oceanographic Office (document number: N6230609PO00123) supported this

study. The authors thank the Naval Oceanographic Office for providing hydrographic data from two seagliders.

Reference

Brainerd, K. E., and M. C. Gregg (1995): Surface mixed and mixing layer depths, *Deep Sea Res., Part A*, **9**, 1521– 1543.

Chu, P.C. (1993): Generation of low frequency unstable modes in a coupled equatorial troposphere and ocean mixed layer. *J. Atmos. Sci.*, **50**, 731-749.

Chu, P.C., C.R. Fralick, S.D. Haeger, and M.J. Carron (1997): A parametric model for Yellow Sea thermal variability. *J. Geophys. Res*., **102**, 10499-10508.

Chu, P.C., Q.Q. Wang, and R.H. Bourke (1999): A geometric model for Beaufort/Chukchi Sea thermohaline structure. *J. Atmos. Oceanic Technol*., **16**, 613-632.

Chu, P.C., C.W. Fan, and W.T. Liu (2000): Determination of sub-surface thermal structure from sea surface temperature. *J. Atmos. Oceanic Technol*., **17**, 971-979.

Chu, P.C., Q.Y. Liu, Y.L. Jia, C.W. Fan (2002): Evidence of barrier layer in the Sulu and Celebes Seas. *J. Phys. Oceanogr*., **32**, 3299-3309.

de Boyer Montegut, C., G. Madec, A.S. Fischer, A. Lazar, and D. Iudicone (2004): Mixed layer depth over the global ocean: an examination of profile data and a profile-based climatology. J. Geophys. Res., **109**, C12003, doi:10.1029/2004JC002378.

Defant, A. (1961): Physical Oceanography, Vol 1, 729 pp., Pergamon, New York.

Kara, A. B., P.A. Rochford, and H. E. Hurlburt (2000): Mixed layer depth variability and barrier layer formation over the North Pacific Ocean. *J. Geophys. Res*., **105**, 16783-16801.

Lindstrom, E., R. Lukas, R. Fine, E. Firing, S. Godfrey, G. Meyeyers, and M. Tsuchiya (1987): The western Equatorial Pacific ocean circulation study. *Nature*, **330**, 533-537.

Lorbacher, K., D. Dommenget, P. P. Niiler, and A. Kohl (2006): Ocean mixed layer depth: A subsurface proxy of ocean-atmosphere variability. *J. Geophys. Res*., **111**, C07010, doi:10.1029/2003JC002157.

Lukas, R. and E. Lindstrom (1991): The mixed layer of the western equatorial Pacific Ocean. *J. Geophys. Res*., **96**, 3343-3357.

Mahoney, K.L., K. Grembowicz, B. Bricker, S. Crossland, D. Bryant, and M. Torres (2009): RIMPAC 08: Naval Oceanographic Office glider operations. *Proc. SPIE*, **Vol. 7317**, 731706 (2009); doi:10.1117/12.820492.

Monterey, G., and S. Levitus (1997): Seasonal Variability of Mixed Layer Depth for the World Ocean, *NOAA Atlas NESDIS 14*, 100 pp., Natl. Oceanic and Atmos. Admin., Silver Spring, Md.

Suga, T., K. Motoki, Y. Aoki, and A. M. Macdonald (2004): The North Pacific climatology of winter mixed layer and mode waters, *J. Phys. Oceanogr.*, **34**, 3 – 22.

Wyrtki, K. (1964): The thermal structure of the eastern Pacific Ocean. *Dstch. Hydrogr. Zeit., Suppl. Ser. A*, **8**, 6-84.

Table 1. Statistical characteristics of H_T identified from the two seagliders using the maximum angle, 0.2°C, 0.5°C, and 0.8°C thresholds.

	Maximum Angle	0.2°C threshold	0.5°C threshold	0.8°C threshold
Mean (m)	77.2	71.9	82.0	87.6
Median (m)	73.2	71.8	77.9	82.9
Standard Deviation (m)	18.3	23.4	18.4	18.0
Skewness	0.69	0.21	1.13	1.25
Kurtosis	3.80	3.48	4.46	4.35

Table 2. Statistical characteristics of H_D identified from the two seagliders using the maximum angle, 0.03 kg/m^3, 0.05 kg/m^3, and 0.125 kg/m^3 thresholds.

	Maximum Angle	0.03 kg/m^3 threshold	0.05 kg/m^3 threshold	0.125 kg/m^3 threshold
Mean (m)	73.2	53.3	59.3	68.0
Median (m)	70.4	60.9	66.2	71.6
Standard Deviation (m)	19.1	32.9	31.0	28.4
Skewness	0.28	-0.06	-0.24	-0.59
Kurtosis	4.32	2.37	2.74	3.67

Table 3. Frequency distributions and RRMSE of calculated isothermal depths from the data consisting of the profile (indicated in Table 1) and random noise with mean of 0 and standard deviation of 0.02^{o} C using the curvature method (without and with 5 point-moving average) and the maximum angle method without smoothing. The total contaminated data profiles are 1000.

Isothermal Layer Depth (m)	Frequency : Curvature (without smoothing)	Frequency: Curvature (with smoothing)	Frequency Maximum Angle (without smoothing)
1	103	0	0
2	125	83	0
3	103	55	0
4	126	44	0
5	98	52	0
6	95	47	0
7	121	43	0
8	105	96	0
9	118	0	0
10	0	3	0
15	0	164	13
20	6	413	987
Total	1000	1000	1000
RRMSE	76%	50%	< 3%

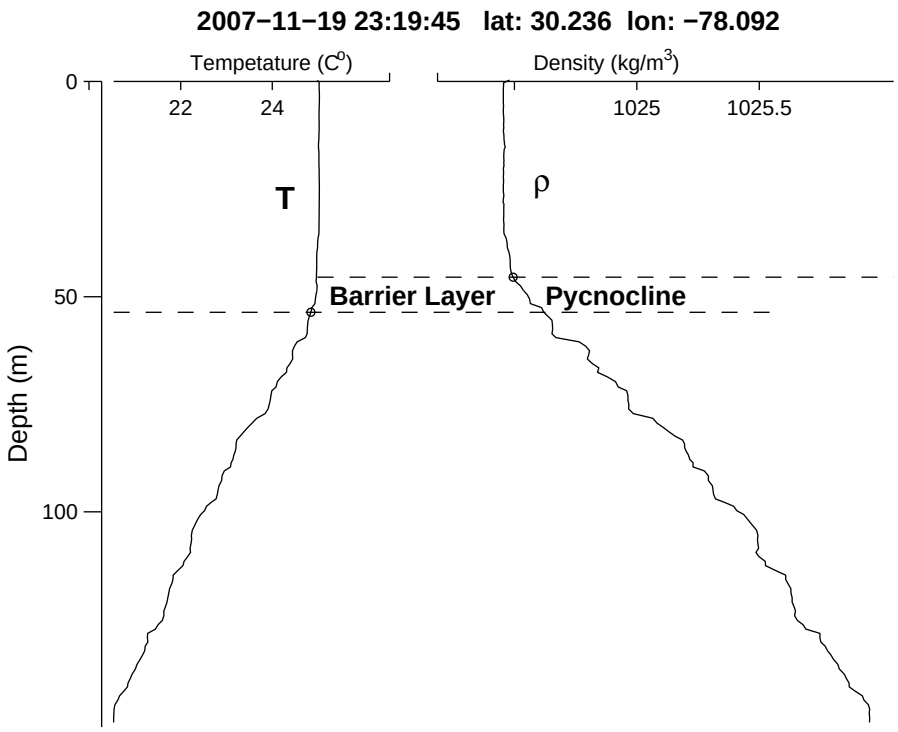

Fig. 1. Isothermal, constant-density, and barrier layers were observed by a seaglider in the western North Atlantic Ocean near the Florida coast (30.236°N, 78.092°W) at GMT 23:20 on November 19, 2007.

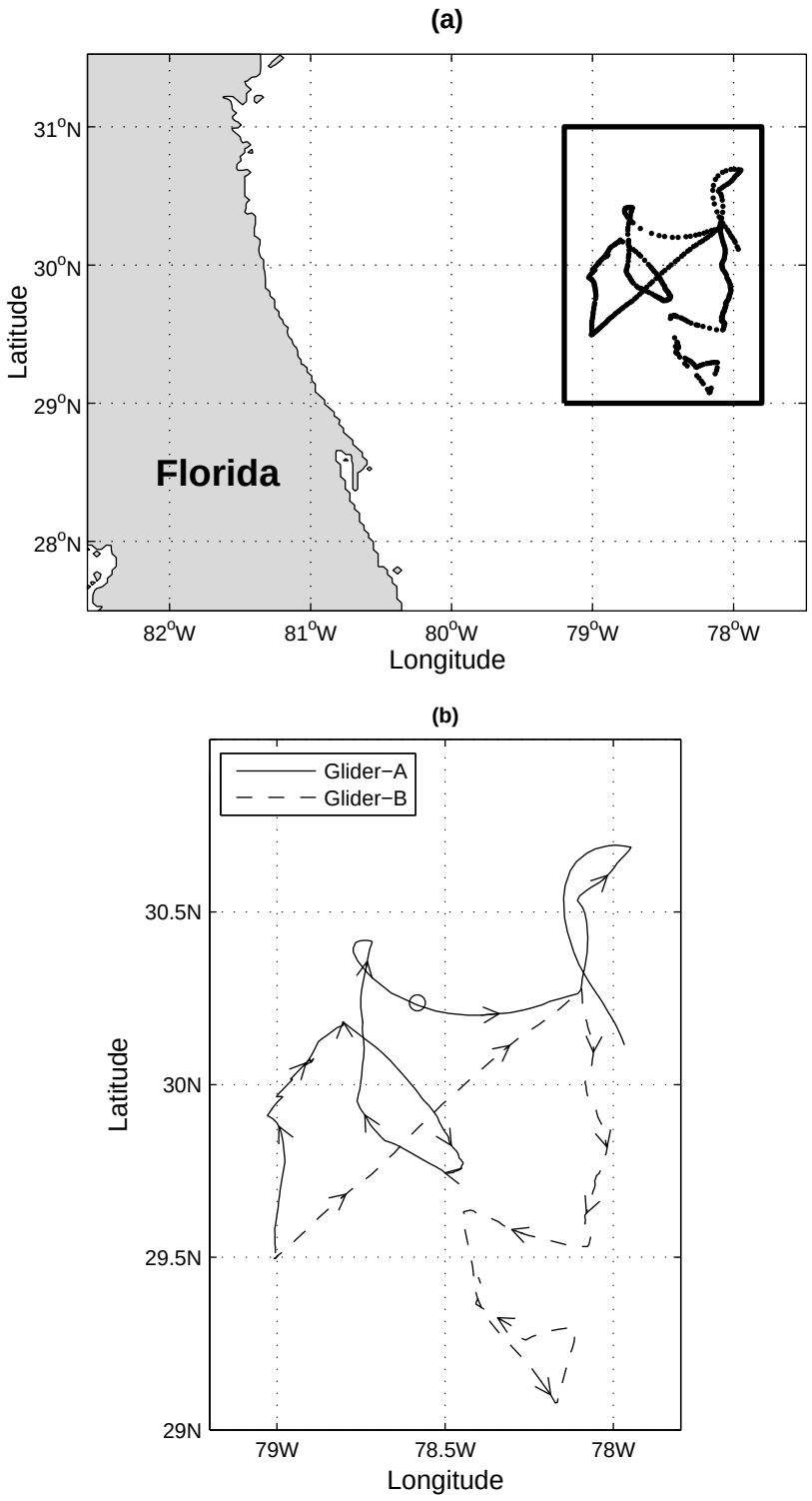

Fig. 2. (a) Location of the glider data, and (b) drifting paths of two gliders with the marked station by circle for demonstration.

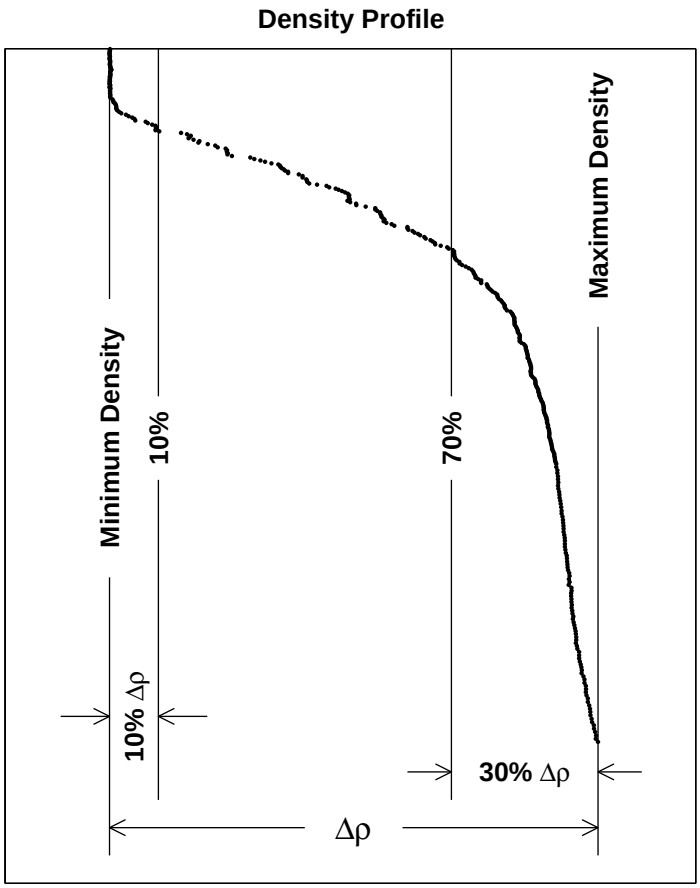

Fig. 3. Illustration for determination of $z_{(0.1)}$ and $z_{(07)}$. There are n data points between $z_{(0.1)}$ and $z_{(07)}$.

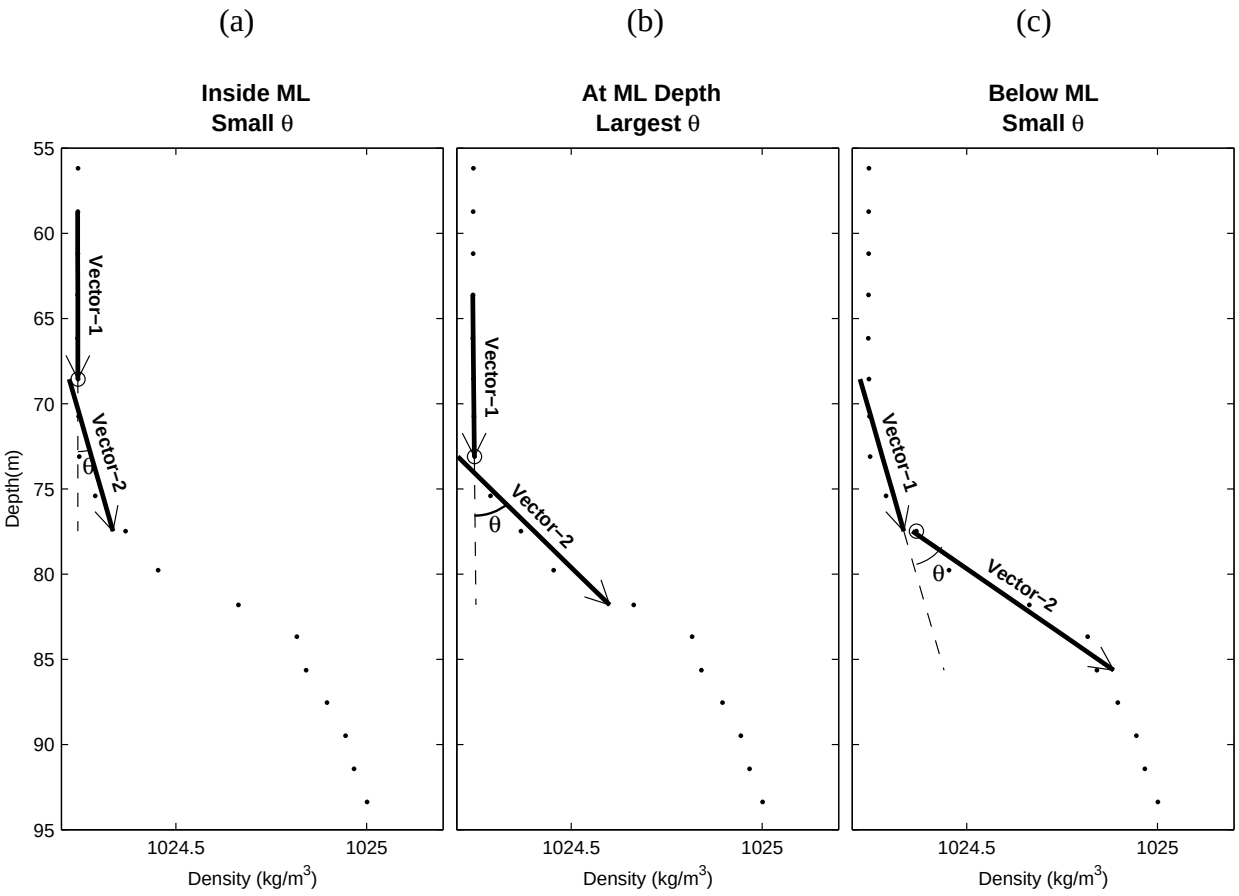

Fig. 4. Illustration of the method: (a) z_k is inside the mixed layer (small θ), (b) z_k at the mixed layer depth (largest θ), and (c) z_k below the mixed layer depth (small θ).

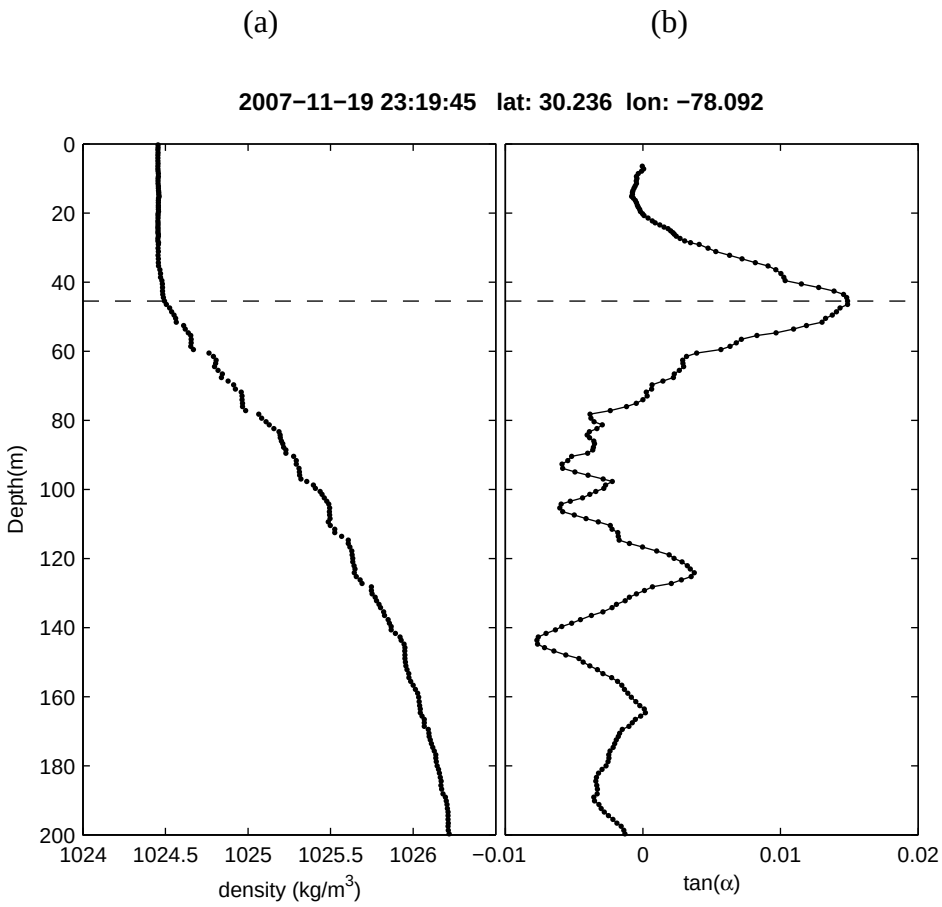

Fig. 5. Determination of H_D using the maximum angle method: (a) density profile at the seaglider station (shown in Fig. 1) located at (30.236°N, 78.092°W) at GMT 23:20 on November 19, 2007, and (b) calculated tan α_k. It is noted that the depth of the maximum tan α_k corresponds to the mixed layer depth and only the upper part of the potential density profile is shown here.

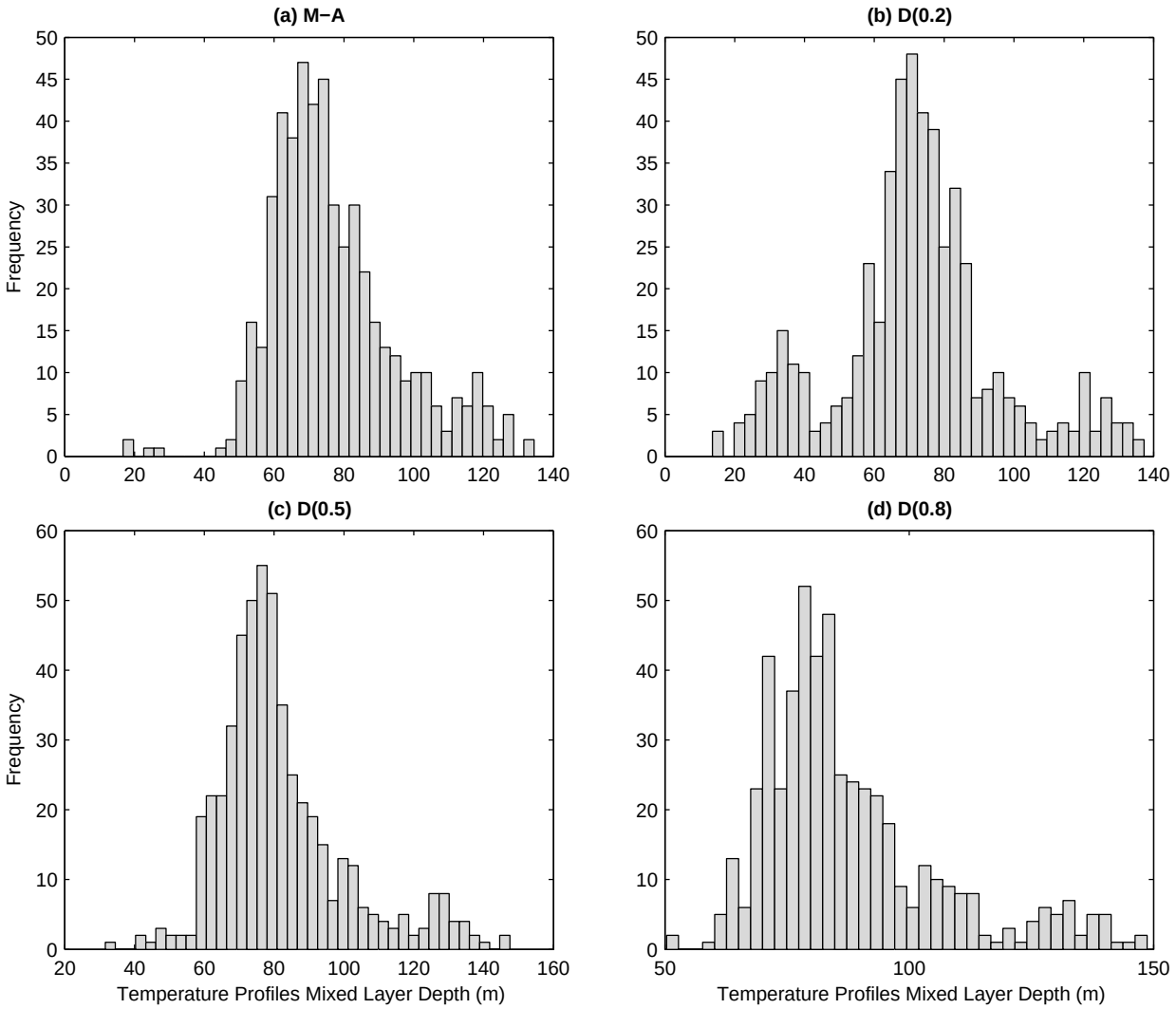

Fig. 6. Histograms of H_T identified using (a) the maximum angle method, (b) 0.2°C, (c) 0.5°C, and 0.8°C difference criteria.

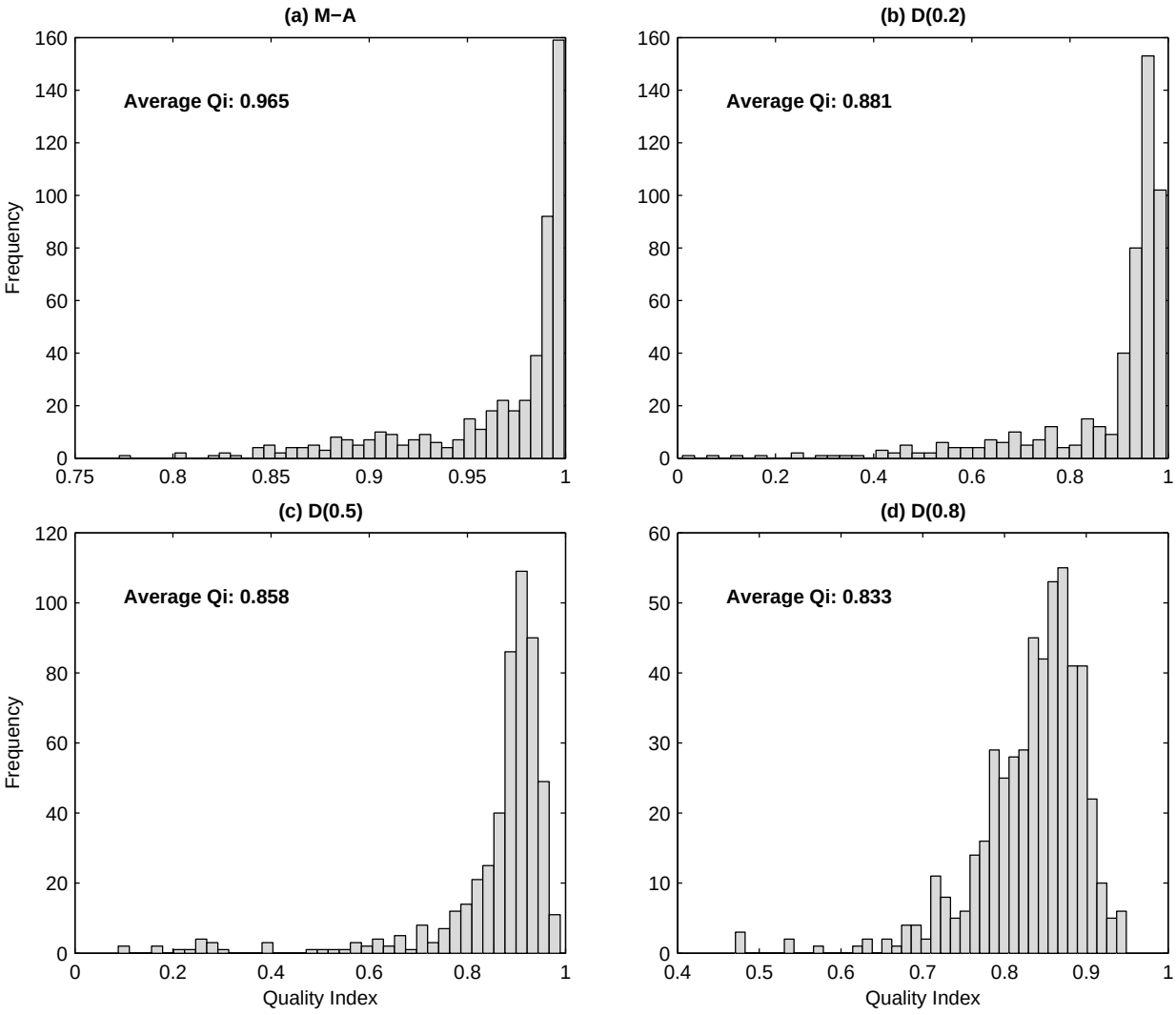

Fig. 7. Histograms of QI using (a) the maximum angle method, (b) 0.2°C, (c) 0.5°C, and 0.8°C difference criteria.

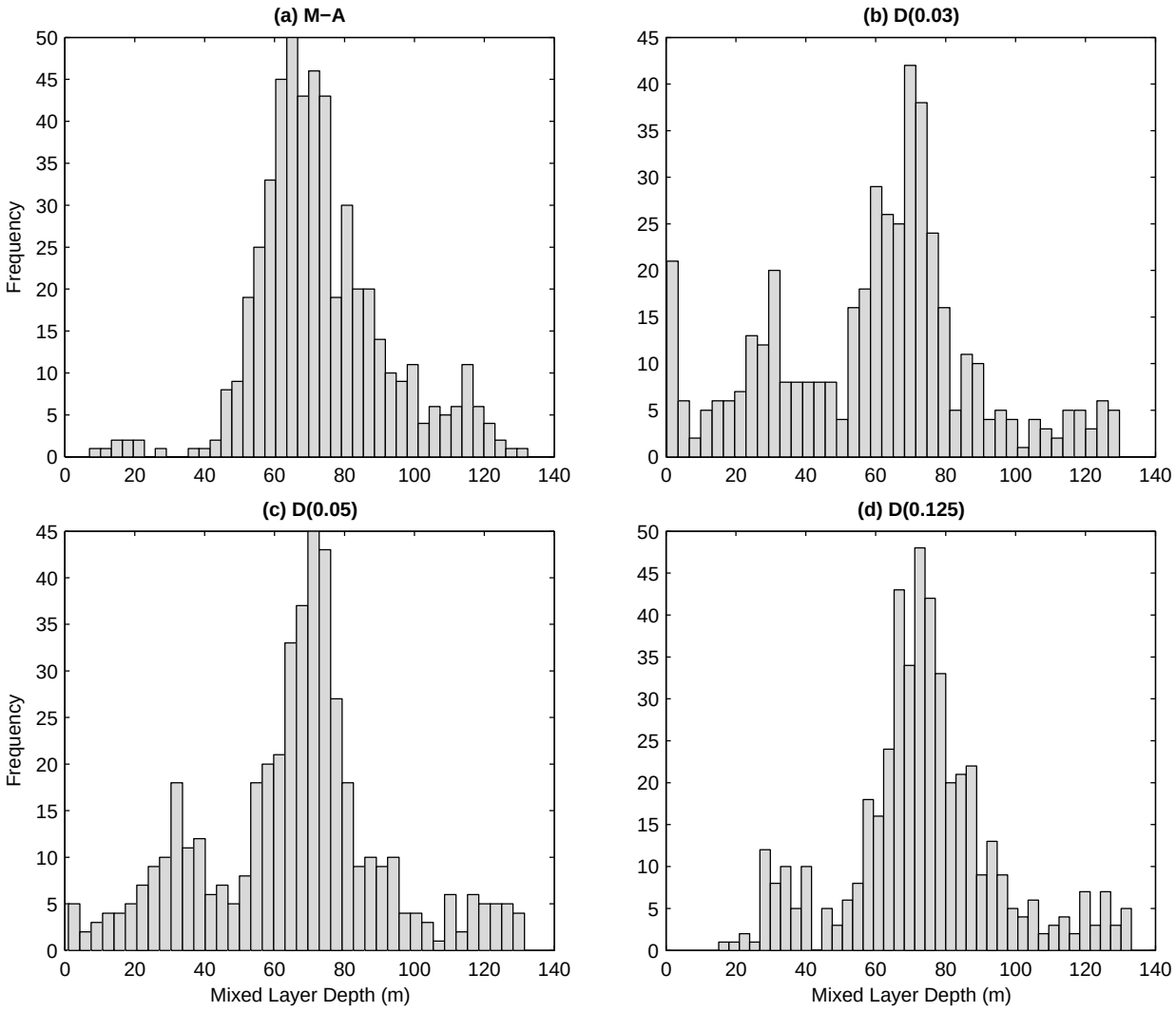

Fig. 8. Histograms of H_D identified using (a) the maximum angle method, (b) 0.03 kg/m^3, (c) 0.05 kg/m^3, and 0.125 kg/m^3 difference criteria.

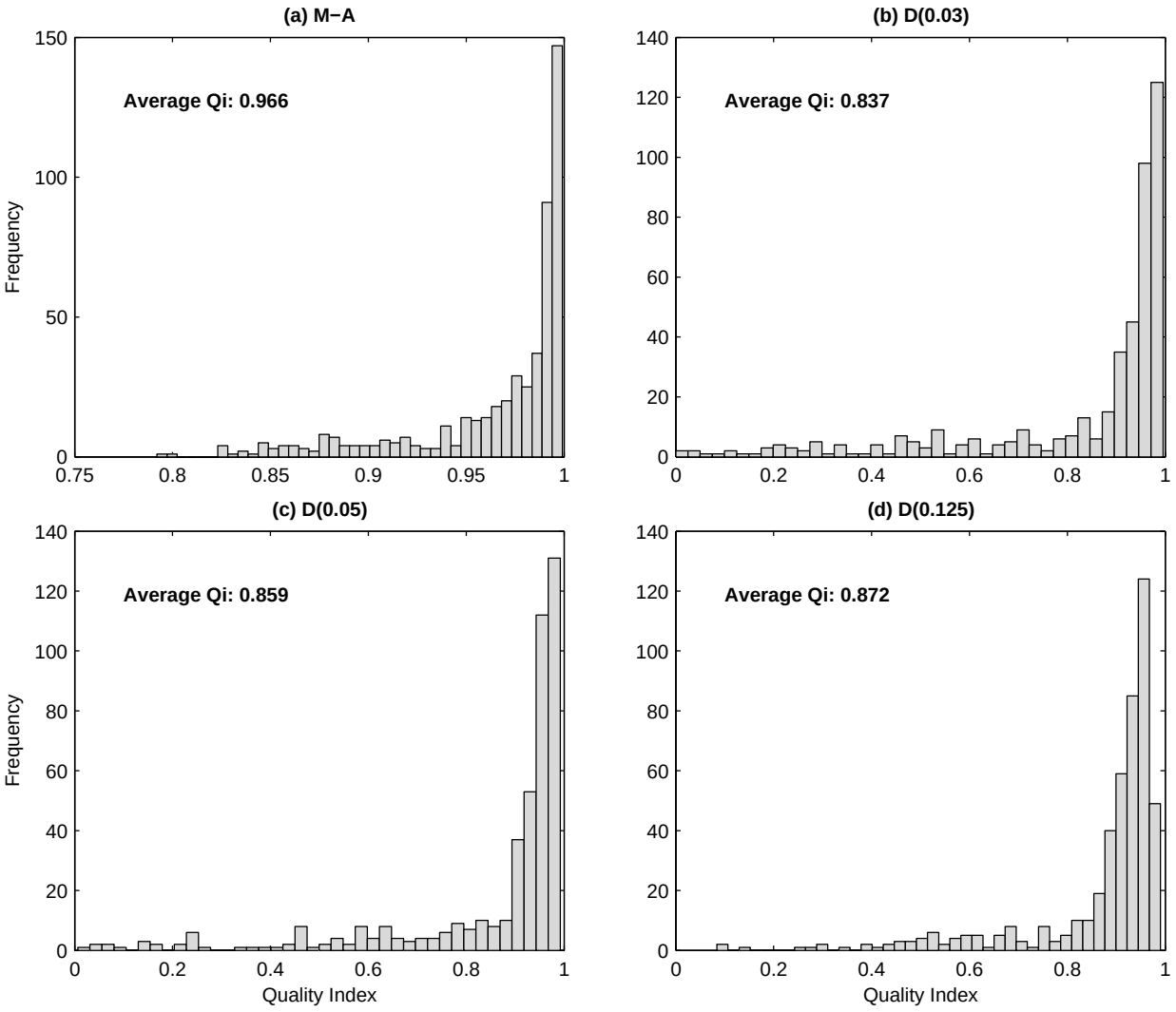

Fig. 9. Histograms of QI using (a) the maximum angle method, (b) 0.03 kg/m^3, (c) 0.05 kg/m^3, and 0.125 kg/m^3 difference criteria.

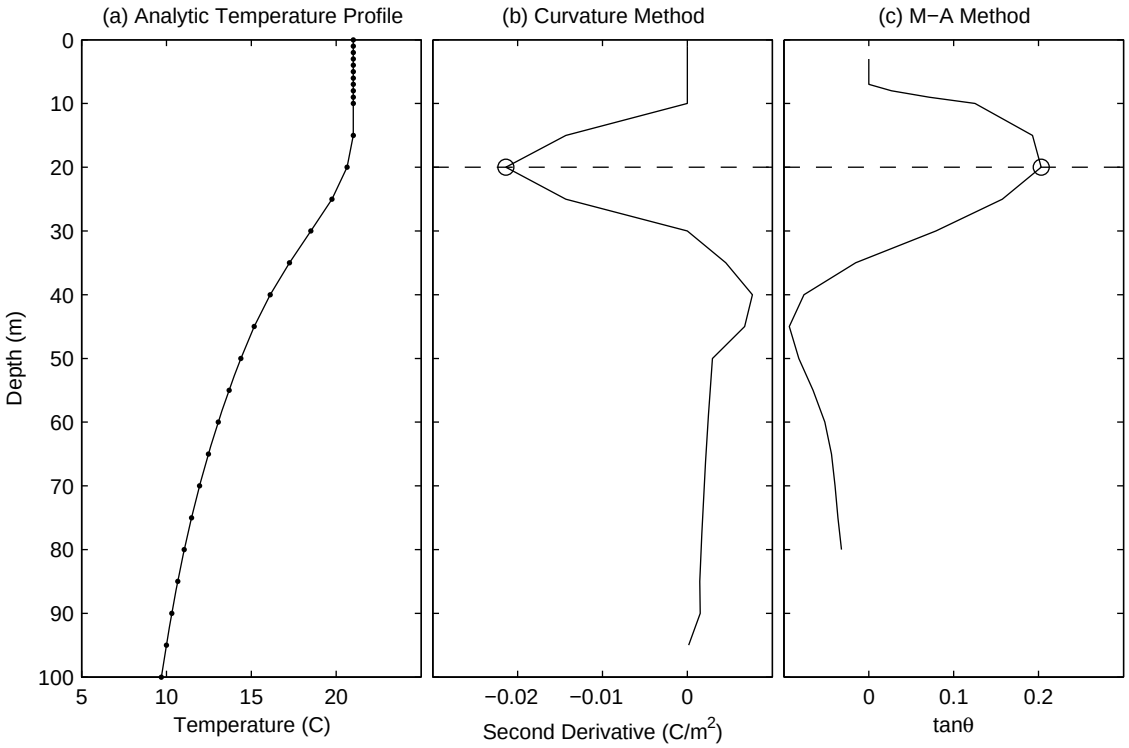

Fig. 10. (a) Smoothed analytic temperature profile (6) by 5-point moving average, calculated (b) $(\partial^2 T/\partial z^2)_k$, and (c) $(\tan\theta)_k$ from the profile data (Fig. 7a). At 20 m depth, $(\partial^2 T/\partial z^2)_k$ has a minimum value, and $(\tan\theta)_k$ has a maximum value.

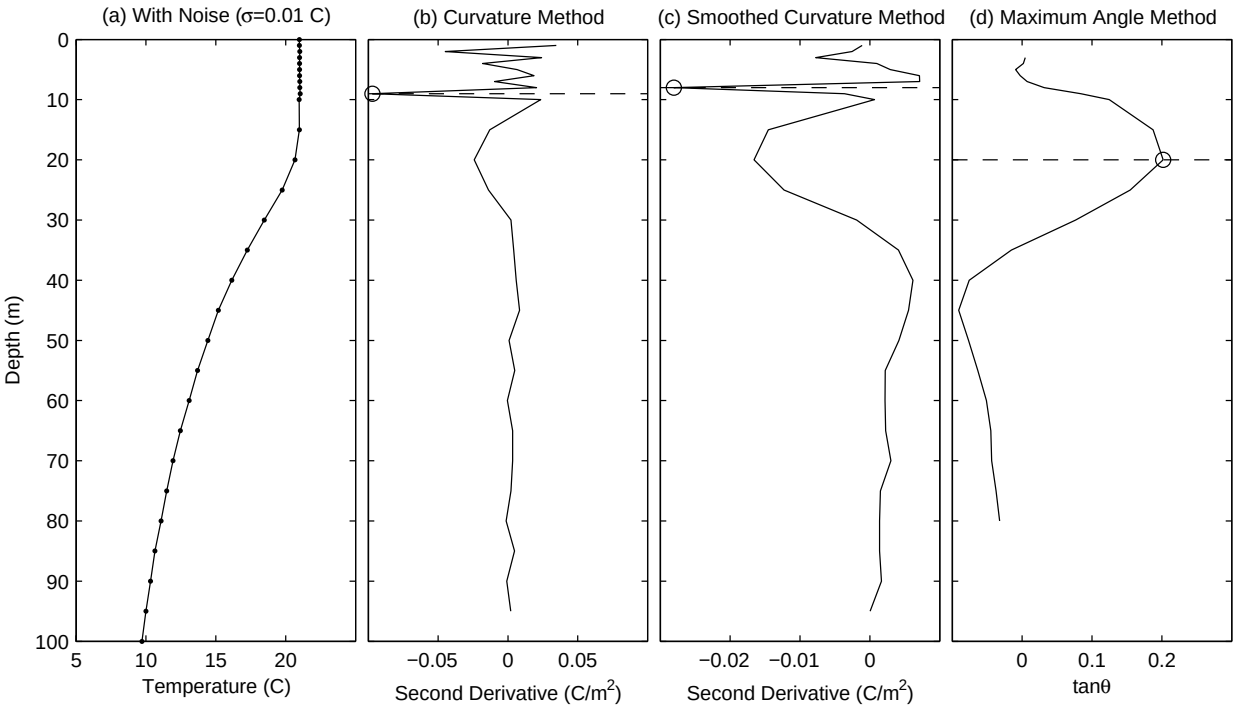

Fig. 11. One out of 1000 realizations: (a) temperature profile shown in Fig. 7a contaminated by random noise with mean of zero and standard deviation of 0.02°C, (b) calculated $(\partial^2 T/\partial z^2)_k$ from the profile data (Fig. 8a) without smoothing, (c) calculated $(\partial^2 T/\partial z^2)_k$ from the smoothed profile data (Fig. 8a) with 5-point moving average, and (d) calculated $(\tan\theta)_k$ from the profile data (Fig. 8a) without smoothing.

(a)

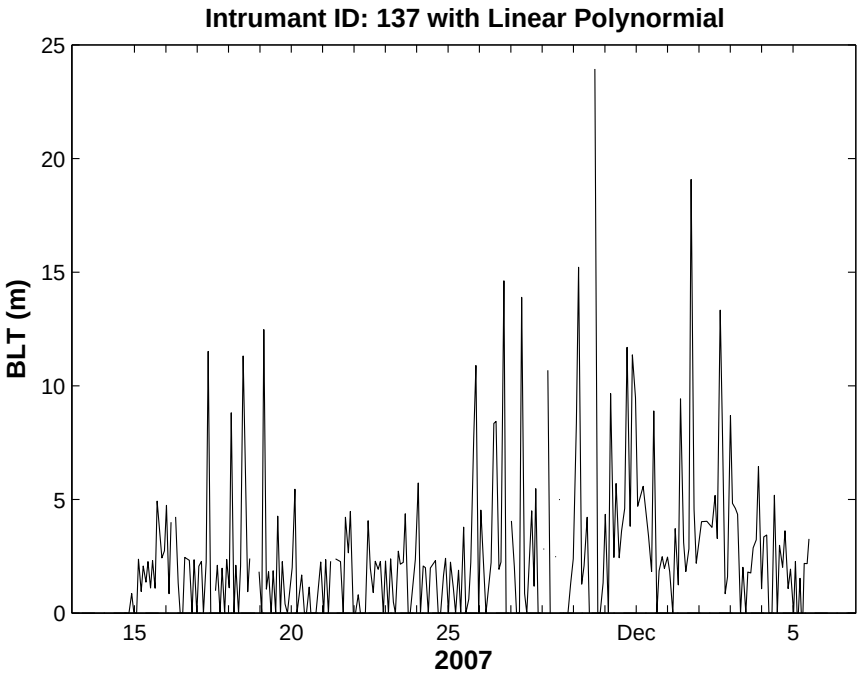

(b)

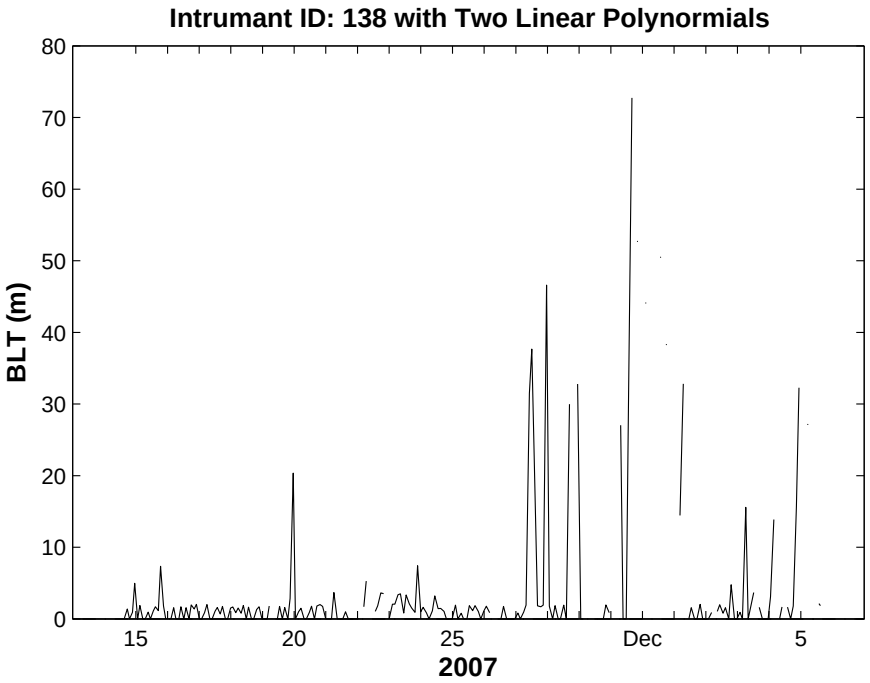

Fig. 12. Temporally varying barrier layer depth identified by the maximum angle method from: (a) Glider-A, and (b) Glider-B.